J Mater Sci: Mater Electron (2016) 27:1553–1557
DOI 10.1007/s10854-015-3923-1

Dielectric properties of ultralow-fired $Mg_4Nb_2O_9$ ceramics co-doped with TiO_2 and LiF

Zhifen Fu[1,2] · Peng Liu[1] · Yi Wu[1] · Baochun Guo[1] · Huaiwu Zhang[3]

Received: 21 August 2015 / Accepted: 17 October 2015 / Published online: 26 October 2015
© Springer Science+Business Media New York 2015

Abstract The $Mg_4Nb_2O_9$ co-doped with 20 wt% TiO_2 (MNT) and x wt% LiF ($1 \leq x \leq 8$) composite ceramics were prepared by a solid-state reaction method for developing ultralow-fired (≤800 °C) microwave dielectric ceramics. The sintering temperatures of MNT ceramics were successfully lowered to 750 °C due to the formation of liquid phase (LiF). A secondary phase of $MgTiO_3$ was observed at above 700 °C for MNT-8 wt% LiF ceramics. All the composite ceramics have the optimal bulk densities at 800 °C, which corresponds to the maximum $Q \times f$ value of 32,000 GHz and ε_r value of 15.7. The well microwave dielectric properties of $\varepsilon_r = 15.6$, $Q \times f = 25{,}000$ GHz, and $\tau_f = -56$ ppm/°C were obtained at 750 °C for 5 h for MNT-8 wt% LiF ceramics. This material is compatible with Ag electrodes, suitable for low-temperature co-fired ceramics applications.

1 Introduction

Low-temperature co-fired ceramics (LTCC) have recently been widely investigated because of the necessity for miniaturization of electronic components and reduction the size of wireless system to achieved integration [1, 2]. A high relative permittivity (≥20) is needed for miniaturization [3], whereas a low relative permittivity ($\varepsilon_r \leq 20$) material is preferred for substrate applications to avoid signal delay [4]. In the past, several microwave dielectric systems, such as Al_2O_3, $MgTiO_3$, Y_2BaCuO_5, Mg_2SiO_4, Mg_2TiO_4, Zn_2SiO_4, $MgAl_2O_4$, have been studied for developing the low dielectric materials. Al_2O_3 filled with La_2O_3–B_2O_3 glass and sintered at 950 °C were reported by Seo et al. ($\varepsilon_r = 8.4$, $Q \times f = 12{,}400$ GHz) [5]. Dai et al. [6] developed a low loss and near zero τ_f LTCC (T2000) based on Al_2O_3 by adding glass and TiO_2 ($\varepsilon_r = 9.1$, $Q \times f = 2500$ GHz). Naoya et al. [7] found that $MgAl_2O_4$ doped with Li–Mg–Zn–B–Si–O glass exhibited low sintering temperatures of 1000 °C and a good microwave dielectric properties ($\varepsilon_r = 7.4$, $Q \times f = 48{,}000$ GHz). Gu [8] and Chen et al. [9] reported that the ultra-low firing $BiVO_4/Li_{0.5}Re_{0.5}WO_4$ (Re = Sm, La, Nd) ceramics with dielectric properties well were obtained.

$Mg_4Nb_2O_9$ (MN) ceramics with a corundum-type structure possesses good microwave dielectric properties ($\varepsilon_r = 12.6$, $Q \times f = 197{,}000$ GHz, $\tau_f = -77$ ppm/°C) at relatively high temperatures (1350–1400 °C) [10–13]. Recently, Lim et al. found that MN exhibited the microwave dielectric properties of $\varepsilon_r = 11.2$, $Q \times f = 15950$ GHz, $\tau_f = 6.7$ ppm/°C at 1300 °C by addition 20 wt% nanosize-TiO_2 [14]. In addition, using the nano-size MN powders produced by high-energy ball milling or chemistry syntheses methods, the sintering temperatures of MN was also decreased lowered [15, 16]. MN nanoceramics were prepared at 1300 °C by high-energy ball milling method and subsequent microwave sintering [17]. Moreover, Zhu et al. [18] reported that the sintering temperatures of MN ceramics were lowered to 1125 °C by using 2 wt% CaO–B_2O_3–SiO_2 glass addition. Additions of Li_2CO_3, V_2O_3, and LiF compounds with low melting temperatures are

✉ Zhifen Fu
18182446920@163.com

✉ Peng Liu
liupeng@snnu.edu.cn

[1] College of Physics and Information Technology, Shaanxi Normal University, Xi'an 710062, China

[2] College of Science, Anhui University of Science and Technology, Huainan 232001, China

[3] The Key Laboratory of Electronic Thin Film and Integrated devices, University of Electronic Science and Technology of China, Chengdu 610054, China

found to be effective in reducing the sintering temperatures of MN ceramics below 960 °C [19]. In the present work, MN doped with nano-size TiO_2 (MNT) and x wt% LiF ($1 \leq x \leq 8$) composite ceramics were prepared by a solid-state reaction method for the development of ultra-low-temperature sintering(≤800 °C) ceramics. The sintering behavior, phase constitutes, microstructures, microwave dielectric properties of MNT ceramics and relationships among them were systematically investigated.

2 Experimental procedure

The starting materials to prepare MN ceramics were MgO (99.99 %, Guo-Yao Co. Ltd., Shanghai, China), Nb_2O_5 (99.99 %, Guo-Yao Co. Ltd., Shanghai, China). They were weighed and milled in a nylon jar with zirconia balls for 7 h, and then dried and calcined at 1000 °C for 10 h. After re-milling with the LiF (≥99.96 %, Guo-Yao Co. Ltd., Shanghai, China) and TiO_2 (rutile structure with a small amount of anatase, purity 99.99 %, and average particle size ca. 80 nm, Guo-Yao Co. Ltd., Shanghai, China) additives, the power was dried, added with of polyvinyl alcohol (PVA), pressed into discs with 11.5 mm in diameter and 5.7 mm in thickness under a pressure of 200 kg/cm^2. Samples were sintered from 700 to 950 °C for 5 h.

The sintering behavior was determined by thermogravimetric analysis (TGA) and differential thermal analyzer (TG/DTA; SDTQ600, USA) with heating rate of 20 °C/min. The bulk densities of the sintered ceramics were measured by Archimedes method. The crystal structures of sintered samples were analyzed by X-ray diffraction (XRD; Rigaku D/MAX2550X, Japan) using CuKα radiation. The microstructures of samples were observed by scanning electron microscopy (SEM; QUANTA200, Holland). The microwave dielectric properties were measured by the Hakki-Coleman dielectric resonator method [20], using a network analyzer (Agilent Tech., HP8720ES). The temperature coefficient of the resonator frequency was also measured by the same method by changing temperatures from 20 to 80 °C and calculated with the following Eq. (1):

$$\tau_f = (f_{80} - f_{20}) \times 10^6/(f_{20} \times 60)\ (\text{ppm}/^\circ\text{C}) \quad (1)$$

where f_{80} and f_{20} were the resonant frequency measured at 80 and 20 °C, respectively.

3 Results and discussion

Figure 1 shows the TG and DTA curves of the MNT doped with 8 wt% LiF. The DTA curve exhibited the four significant peaks, noted as points A, B, C and D, respectively. At around 200 °C (point A), one endothermic peak was observed consistent with the loss of water in the first weight loss. The exothermic peak (point B) is due to decomposition of PVA accompany with the second weight loss at around 300 °C. The endothermic peaks appeared at 480 °C (point C) is corresponding to transformation of nano-sized TiO_2 crystal structure from the polymorphic anatase to rutile [21], and the peak D at 750 °C is related to the melting of LiF compound. These results provide evidence of helping sintering MN ceramics as shown below.

Powders XRD patterns of MNT specimens with 8 wt% LiF sintered at 500–950 °C for 5 h are shown in Fig. 2. The peaks were indexed to be MN (JCPDS #38-1459) and TiO_2 phases with a minor of LiF phase at the temperatures ranging from 500 to 650 °C. For the specimens sintered at temperatures exceeding 700 °C, an impurity ilmenite phase $MgTiO_3$ was detected (JCPDS #79-0831), accompanying with the disappearing of TiO_2 and LiF phases. Thus, the chemical reaction (2) should occur at temperatures ≥600 °C:

$$Mg_4Nb_2O_9 + 4TiO_2 = 4MgTiO_3 + Nb_2O_5 \quad (2)$$

In addition, as shown in Fig. 2, with an increase of sintering temperatures, LiF phase gradually was disappeared at temperatures higher than 700 °C due to the evaporation of LiF or existence in amorphousness.

The MNT specimens doped with various LiF and sintered at 750 °C for 5 h are shown in Fig. 3. MN, TiO_2, $MgNb_2O_6$ phases are detected in the specimens with 1 wt% LiF. With increasing LiF content from 1 to 8 wt%, the peak intensity of $MgTiO_3$ phase increase accompany with disappearing of $MgNb_2O_6$ and TiO_2 phases. Thus, the chemical reaction (3) was supposed to occur:

$$MgNb_2O_6 + TiO_2 = MgTiO_3 + Nb_2O_5 \quad (3)$$

As shown in the inset of Fig. 3, compared with pure MN phase, the 2θ values of the strongest diffraction peak (104)

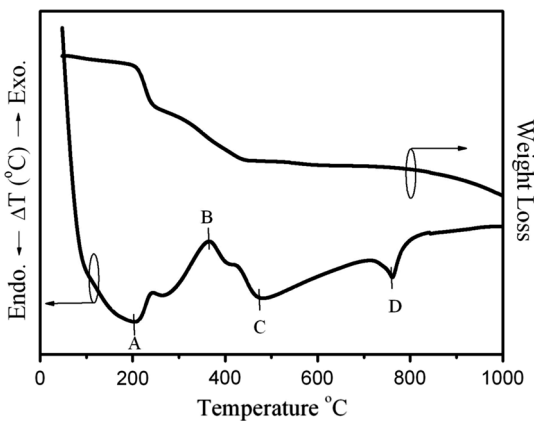

Fig. 1 TG-DTA *curves* of MNT with 8 wt% LiF

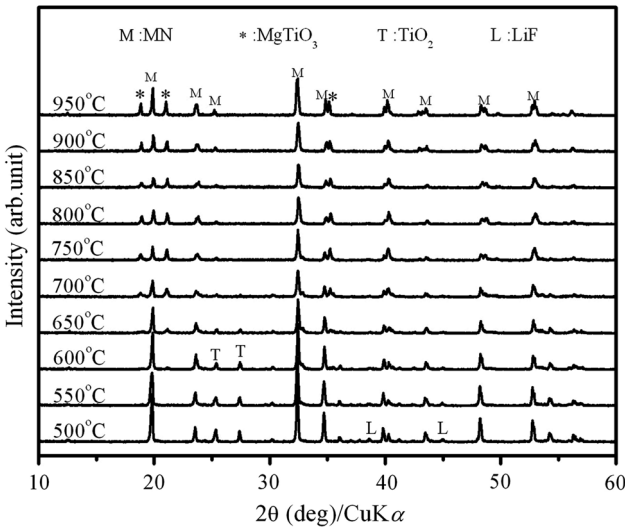

Fig. 2 XRD patterns of MNT with 8 wt% LiF sintered at various temperatures for 5 h

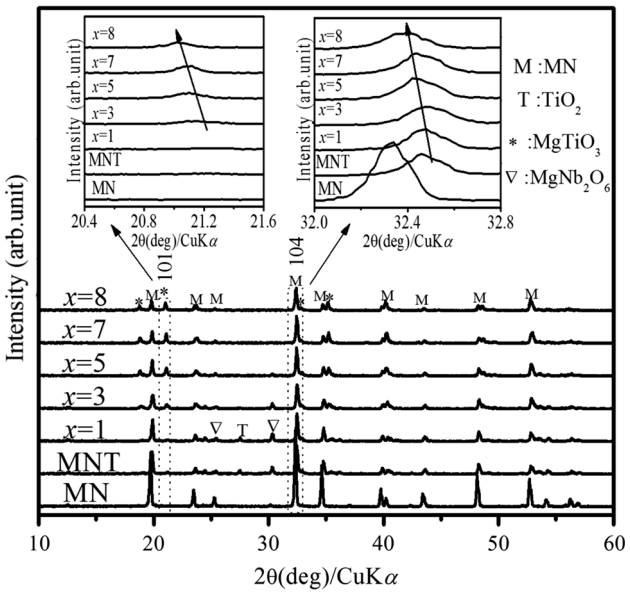

Fig. 3 XRD patterns of MNT with x wt% LiF ($x = 1, 3, 5, 7, 8$ wt%) sintered at 750 °C

of MNT phase obviously shifted from 32.25° to 32.55°, due to some of Ti^{4+} ions (ionic radius = 0.605 Å, coordination number CN = 6) enter the Nb^{5+} (0.64 Å, CN = 6) site. Moreover, with LiF content increasing from 1 to 8, (104) peak turns toward the lower angles, which is related to a substitution of larger Li^{+} (0.76 Å, CN = 6) for Mg^{2+} (0.72 Å, CN = 6) site of MN, as we ever discussed in [15]. Finally, the (101) peak positions of $MgTiO_3$ phase shift to lower angles with increasing LiF content, implying that Nb^{5+} ions originating from reactions (2) and (3) enter the Ti^{4+} site or Li^{+} ions substitute Mg^{2+} of $MgTiO_3$ compound. The chemical reactions and ion diffusions process taking place among MN, TiO_2, and LiF compounds during the sintering process strongly depend on the temperatures, powder size, and other processing factors. The chemical reactions provide the best wetting condition of MN powders, and MNT can be sintered by a liquid sintering process at low temperatures [22].

SEM pictures of fractured surface of the MNT ceramics with 8 wt% LiF additions sintered at 700–950 °C are shown in Fig. 4. It shows that the grains grew and congregated evidently as increasing sintering temperatures. All samples showed porous microstructures, which may be related to volatilization of LiF [23]. For the samples sintered at 800 °C, the average grain sizes reached the minimum values (~700 nm). The energy dispersive spectroscopy (EDS) analysis of the specimens sintered at 750 °C showed that the dark phase primarily contained Mg, Nb, O and small amounts of Ti elements, while the white phase contained more amounts of Ti element than the deep-color phase. Thus, the dark regions are mainly composed of MN phase and the $MgTiO_3$ phase was mainly in the white regions. The inter-diffusion occurred between the two phases during firing process, resulting in a shift of XRD peak positions of both MN and $MgTiO_3$ phases as shown in Fig. 3.

Figure 5 shows the bulk densities (ρ), dielectric constants (ε_r) and $Q \times f$ values of MNT ceramics doped with LiF as a function of sintering temperatures. As shown in Fig. 5a, all the sintered samples have their optimal bulk densities at about 800 °C except specimens with 5 wt% LiF, corresponding to their maximum $Q \times f$ values and the maximum dielectric constant in Fig. 5b, c. This is due to a high density and a low porosity which leads to a high dielectric constant and $Q \times f$ value [24]. The densification of ceramics at low temperatures originated from the formation of liquid phase LiF as sintering agent (Fig. 1). In Fig. 5b, the higher ε_r values than that of pure MN ($\varepsilon_r = 12.6$) are related to the existence of $MgTiO_3$ phase ($\varepsilon_r = 17.17$) [24]. The variation of $Q \times f$ value is affected by many factors such as lattice irrational modes, porous, grain boundaries, and secondary phases [25]. In Fig. 5c, $Q \times f$ values of all compositions have the maximum values at 800 °C, which is in agreement with their highest densities. With an increase of temperature from 800 to 950 °C (seen in Fig. 2), the decrease of $Q \times f$ values may be due to an increase of $MgTiO_3$ phase ($Q \times f = 20{,}780$ GHz) [24]. Since the smallest average grain size (~700 nm) is observed for the MNT ceramics sintered at 800 °C (Fig. 4c), the dielectric loss of MNT ceramics is supposed to be mainly caused by the porous and secondary phases rather than grain boundaries, similar to that ever found in Al_2O_3, MgO, and $LaAlO_3$ dielectric materials [26, 27]. In addition, the oxygen vacancy and lattice defects, which are caused by the substitution of Li^{+} for Mg^{2+} and Ti^{4+} for

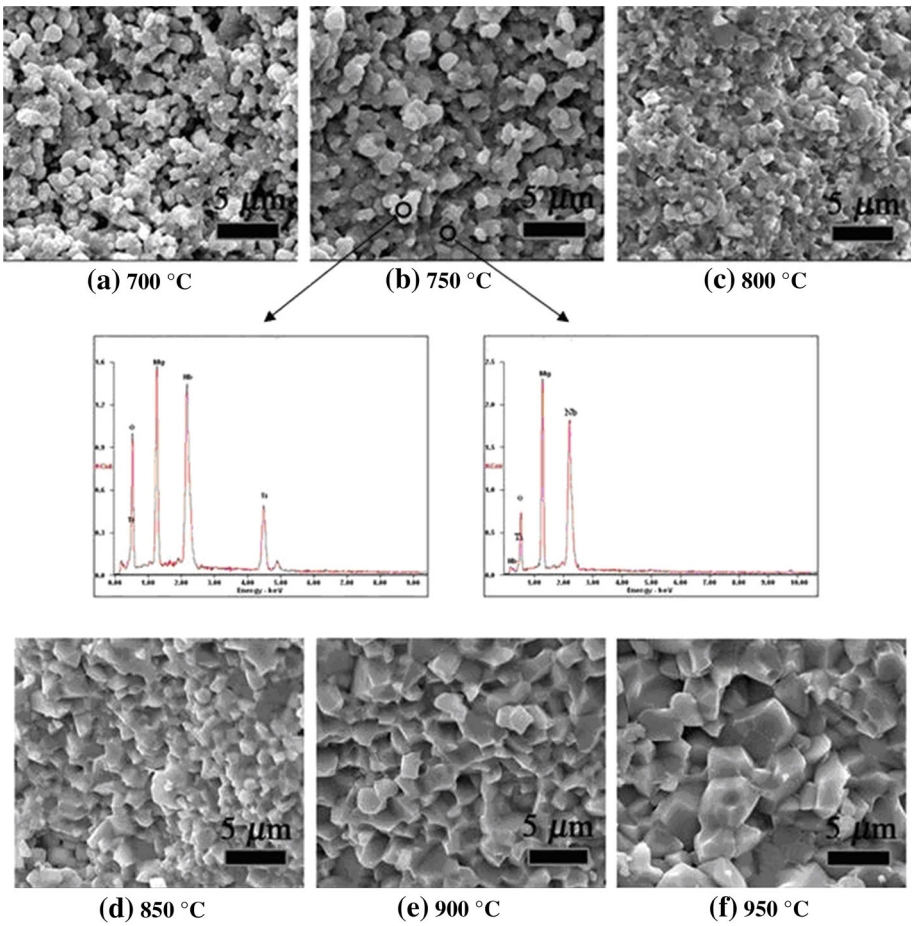

Fig. 4 SEM of fractured surface of the MNT ceramics with 8 wt% LiF additions sintered from 700 to 950 °C for 5 h

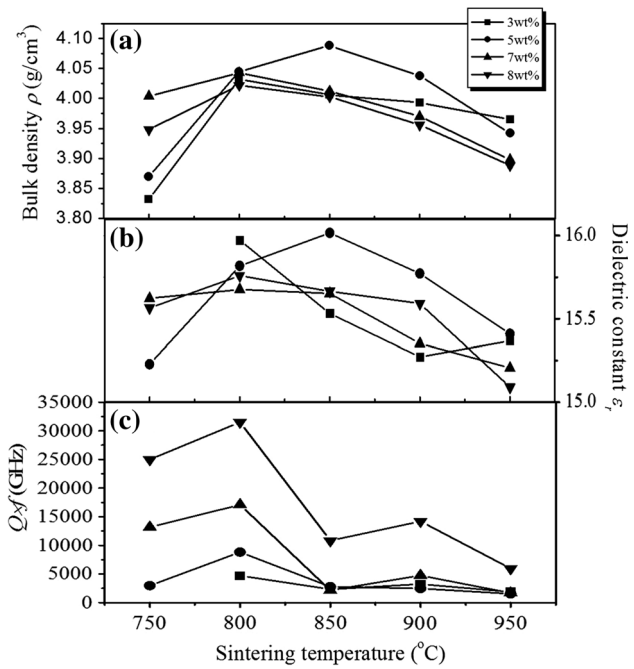

Fig. 5 Bulk density, ε_r value and $Q \times f$ value of MN with 20 wt% TiO_2 and x wt% LiF ($x = 1, 3, 5, 7, 8$ wt%) sintered at various temperatures for 5 h

Nb^{5+} in the solid solution of $(Mg,Li)_4(Nb,Ti)_2O_{9-\delta}$ (confirmed by Fig. 3), should also contribute to the decrease of $Q \times f$ values.

The temperature coefficient resonant frequency of MNT with 8 wt% LiF content is not tuned appropriately (−56 ppm/°C) because of the small τ_f value of secondary phase $MgTiO_3$ (−50 ppm/°C) [24].

Figure 6 shows the XRD patterns of mixtures (MNT powders with 8 wt% LiF and Ag powders) and that after heat-treated at 800 °C. None impurity phases were observed in the XRD patterns, demonstrating a good chemical compatibility between the MNT-8 wt% LiF ceramics and Ag.

4 Conclusions

The $Mg_4Nb_2O_9$ co-doped with 20 wt%TiO_2 (MNT) and x wt% LiF ($1 \leq x \leq 8$) composite ceramics were primarily prepared by a solid-state reaction method. It was found that addition of 8 wt% LiF and 20 wt% TiO_2 effectively reduced the sintering temperature of $Mg_4Nb_2O_9$ ceramics from 1400 to 750 °C due to the formation of liquid phase

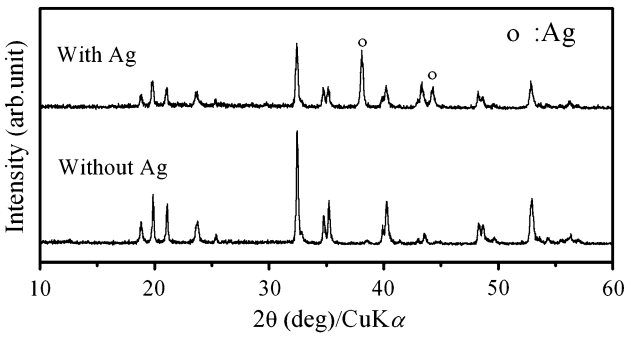

Fig. 6 XRD patterns of MNT with 8 wt% LiF ceramics and mixture of MNT with 8 wt% LiF ceramic and Ag heat-treated at 750 °C for 5 h in air

(LiF). The grain size of MNT-8 wt% LiF ceramics grew as the increasing sintering temperatures and a secondary phase $MgTiO_3$ was formed due to a chemical reaction between MN and TiO_2 compounds. All the samples had optimal bulk densities at about 800 °C, which is corresponds to the maximum $Q \times f$ value of 32,000 GHz and the maximum dielectric constant of 15.7. The decrease of $Q \times f$ values MNT ceramics are related to the formation of lattice defects, porous, and secondary phases rather than grain boundaries. The MNT specimens with 8 wt% LiF sintered at 750 °C had the good microwave dielectric properties of $\varepsilon_r = 15.6$, $Q \times f = 25{,}000$ GHz, and $\tau_f = -56$ ppm/°C. The good compatibility of MNT ceramics with Ag makes it a suitable candidate for LTCC application.

Acknowledgments This work is supported by the National Natural Science Foundation of China (Grant Nos. 51272150, 51572162 and 51132003), the Scientific Research Foundation of Shaanxi Normal University (Grant No. X2013YB01), Specialized Research Fund for the Doctoral Program of Higher Education (No. 20120202110004), and the Fundamental Research Funds for the Central Universities (GK201401003).

References

1. N.X. Xu, J.H. Zhou, H. Yang, Ceram. Int. **40**, 15191–15198 (2014)
2. G.G. Yao, P. Liu, H.W. Zhang, J. Am. Ceram. Soc. **96**, 1691–1693 (2013)
3. K.W. Long, K.M. Luk, Int. J. Antennas. Propag. **43**, 517–519 (1995)
4. R.R. Tummala, J. Am. Ceram. Soc. **74**, 895–908 (1991)
5. Y.J. Seo, D.J. Shin, Y.S. Cho, J. Am. Ceram. Soc. **89**, 2352–2355 (2006)
6. S.X. Dai, R.-F. Huang, D.L. Wilcox, J. Am. Ceram. Soc. **85**, 828–832 (2002)
7. N. Mori, Y. Sugimoto, J. Harada, Y. Higuchi, J. Eur. Ceram. Soc. **26**, 1925–1928 (2006)
8. F.F. Gu, G.H. Chen, X.L. Kang et al., J. Mater. Sci. **50**, 1295–1299 (2015)
9. G.H. Chen, F.F. Gu, M. Pan et al., J. Mater. Sci. Mater. Electron. **26**, 6511–6517 (2015)
10. N. Kumada, K. Taki, N. Kinomura, Mater. Res. Bull. **35**, 1017–1021 (2000)
11. A. Kan, H. Ogawa, A. Yokoi, Y. Nakamura, J. Eur. Ceram. Soc. **27**, 2977–2981 (2007)
12. A. Kan, H. Ogawa, A. Yokoi, Mater. Res. Bull. **41**, 1178–1184 (2006)
13. H. Ogawa, A. Kan, S. Ishihara, Y. Higashida, J. Eur. Ceram. Soc. **23**, 2485–2488 (2003)
14. C.L. Huang, J.Y. Chen, C.C. Liang, Mater. Res. Bull. **44**, 1111–1115 (2009)
15. Z.F. Fu, P. Liu, X.M. Chen et al., J. Alloys Compd. **493**, 441–444 (2010)
16. H.T. Wu, L.X. Li, Q. Zou et al., J. Alloys Compd. **509**, 2232–2237 (2011)
17. M.H. Sarrafi, H.B. Bafrooei, M. Feizpour et al., J. Mater. Sci. Mater. Electron. **25**, 946–951 (2014)
18. H. Zhu, W. Shen, Y. Jin et al., J. Mater. Sci. Mater. Electron. **24**, 3546–3550 (2013)
19. A. Yokoi, H. Ogawa, A. Kan, H. Ohsato, Y. Higahsida, J. Eur. Ceram. Soc. **25**, 2871–2875 (2005)
20. B.W. Hakki, P.D. Coleman, IRE Trans. Microwave Theory Tech. **8**, 402–410 (1960)
21. A.A. Gribb, J.F. Banfield, Am. Mineral. **82**, 717–728 (1997)
22. M.J. Wang, H. Yang, Q.L. Zhang et al., J. Mater. Sci. Mater. Electron **26**, 162–167 (2015)
23. X.M. Wu, S. Chen, Z.Q. He et al., Thin Solid Films **589**, 574–577 (2015)
24. L. Li, X.M. Chen, X.C. Fan, J. Eur. Ceram. Soc. **26**, 3265–3271 (2006)
25. Q.L. Zhang, H. Yang, J.L. Zou, H.P. Wang, Mater. Lett. **59**, 880–884 (2005)
26. S.J. Penn, N.M. Alford, A. Templeton et al., J. Am. Ceram. Soc. **80**, 1885–1888 (1997)
27. J.D. Breeze, J.M. Perkins, D.W. McComb et al., J. Am. Ceram. Soc. **92**, 671–674 (2009)